TDA Progress Report 42-85

January–March 1986



# Total Ionospheric Electron Content Calibration Using SERIES GPS Satellite Data

G. Lanyi
Tracking System and Applications Section

*This article describes the current status of the Deep Space Network advanced systems research into ionospheric calibration techniques, based on Global Positioning System (GPS) data. A GPS-based calibration system is planned to replace the currently used Faraday rotation method by 1989. The SERIES receiver system used in this research determines the differential group delay of signals transmitted at two different carrier frequencies. This differential delay includes an ionospheric component and a GPS transmitter offset. The transmitter offsets are different for each GPS satellite. Tests have been conducted to assess the effect of the offsets on the ionospheric calibration accuracy. From the obtained data, the total electron content and GPS transmitter offsets are calculated by a least-squares estimation method employing a local model of total ionospheric electron content. The end product is an estimation of the total ionospheric content for an arbitrary line-of-sight direction. For the presented polynomial fitting technique, the systematic error due to mismodeling is estimated to be* $\sim 6 \times 10^{16}$ *el/m*$^2$*, while the formal error is* $\sim 2 \times 10^{16}$ *el/m*$^2$*. The final goal is an error of* $3 \times 10^{16}$ *el/m*$^2$ *(~0.7 ns at 2.3 GHz).*

## I. Introduction

Electromagnetic waves traversing the Earth's ionosphere are delayed due to refractive properties of the ionosphere. For precise deep-space navigation, the calibration of the ionospheric delay is a required procedure. Also, certain radio-science experiments on space missions rely on precise calibration of the terrestrial total ionospheric electron content.

The Deep Space Network (DSN) monitors the ionospheric total electron content (TEC) by a Faraday rotation technique utilizing polarization of radio signals transmitted by quasi-geostationary satellites (Ref. 1). The Faraday receivers are in the proximity of the DSN antennas. The line-of-sight TEC in the direction of a space probe to be calibrated is estimated from Faraday measurements by the program DIEN/TIEN described in Ref. 2. In the present DSN configuration, this algorithm estimates with an error of ~10%, in the worst case, resulting in an error of $30 \times 10^{16}$ el/m$^2$. Due to the declining number of Faraday satellites and increasing precision requirements for ionospheric calibration, the DSN plans to implement a Global Positioning Satellite (GPS)-based ionospheric calibration system (Ref. 3). The planned receiver network will also perform precise clock synchronization between the DSN stations. The following is a description of the GPS-based ionospheric calibration technique under consideration.

Presently, ionospheric delay data are obtained by the proof-of-concept SERIES and SERIES-X receivers developed by the Jet Propulsion Laboratory (Refs. 4, 5, and 6).[1] Here we report results obtained from SERIES data only, and SERIES-X data will be analyzed in the future. The ionospheric delays are obtained by measuring the differential arrival times of the P-code signals at L1 and L2 frequencies (Fig. 1). With the current GPS configuration, the SERIES receiver scans 5 satellites in a sequential manner, obtaining one 2-s observation per minute, for a total of ~300 observations in a 5-h observing session. The GPS observations cover only certain regions of the sky and the line of sight of a space probe to be calibrated might not overlap with the GPS observations. Therefore, in order to be able to estimate the total electron content at an arbitrary line-of-sight direction from the SERIES data, specific assumptions have to be made about the behavior of the ionosphere. We assume that the electron content is time independent for the duration of the observation session in a geocentric solar reference frame oriented along the Earth-Sun axis. This is to say that the electron distribution produced by ionization due to solar radiation (Ref. 7) is assumed to be in equilibrium and we deal with only the static part of electron density redistributed by the Earth's magnetic field. We then approximate the electron content by a second-order polynomial in the Earth-centered solar spherical coordinates for a given observation session. In other words, the functional form of the total ionospheric content is assumed to be a static paraboloid in coordinates of geocentric solar latitude and longitude where the origin of the coordinate system corresponds approximately to the middle of the observing session. The ionospheric region corresponding to an observing session spans ~15 deg in latitude and ~90 deg in longitude. The electron content parameters and GPS satellite offsets (see the description of transmitter errors in Appendix A) are determined by least-squares estimation. The separation of GPS transmitter offsets from effects due to ionosphere is facilitated by the dependence of ionospheric path delay on the elevation angle of observations.

The electron content, however, is only approximately time-independent in the chosen geocentric solar reference frame. Time-dependent effects are not modeled at present, though semiempirical estimation of some of these effects may be possible. In order to avoid possible confusion, we should note here that the typical diurnal variation observed in the terrestrial reference frame (Fig. 2) is due primarily to the fact that the observer looks at different points on the static ionospheric shell as the Earth rotates. On the other hand, the time-variation effect in the solar reference frame is a correction to the static approximation of the ionosphere.

Ionospheric fluctuations due to inhomogeneities result in high-frequency temporal and spatial variations and the modeling of this effect could prove to be formidable. Consequently, with the current technique, the formal error of ionospheric estimation is always larger than the root-mean-square (rms) scatter of ionospheric fluctuations, unless the angular separation between the direction of prediction and observation is very small.

In order to demonstrate the capabilities of the static-model calibration algorithm, we display the errors due to all sources in a bar chart in Fig. 3. The first bar on the left represents the effect of uncertainties in the estimation of GPS transmitter offsets, and the next bar is primarily the sum of receiver calibration error and multipath effects. The third bar estimates the effect of ionospheric fluctuations and the following bar represents the ionospheric mapping errors. The last bar gives a summary of the line-of-sight ionospheric calibration error.

The experimental formal error of $1.5 \times 10^{16}$ el/m$^2$ corresponds approximately to the rss of the transmitter and receiver errors and inhomogeneities; the modeling error is largely systematic in nature. The presented error budget assumes properly calibrated receivers and the GPS transmitter offset estimation. A more detailed description of these error sources is given in Appendix A.

In the following sections we will give a brief description of the estimation technique and experimental results. Section II will discuss the modeling and estimation techniques, and in Section III the results of this estimation will be presented. In Section IV, in addition to the summary of results, the possible improvements and additions will be discussed.

Finally, we should point out that while we are estimating total electron content, the instrument measures the difference in P-code group delays of transmission at L1 = 1.57542 GHz and L2 = 1.2276 GHz frequencies. Both of these quantities, TEC and differential delays, will be referenced in the text and figures. The physically measured delay will be in the units of nanoseconds (ns) and the TEC will have the units of electrons/meter$^2$ (el/m$^2$). The conversion between these units is 1 ns = $2.8 \times 10^{16}$ el/m$^2$.

## II. Modeling and Statistical Estimation

Prediction of the ionospheric electron content along an arbitrary line of sight is difficult due to the complexity of underlying physical phenomena. Therefore, most prediction

[1] See also Crow, R. B., Bletzacker, F. R., Najarian, R. J., Purcell, Jr., G. H., Statman, J. I., and Thomas, J. B., SERIES-X *Final Engineering Report*, JPL D-1476 (JPL internal document), Jet Propulsion Laboratory, Pasadena, Calif., 1984.

techniques are semiempirical in nature; semiempirical ionospheric electron content parameters are determined by the use of a large number of global ionospheric sounding data supplemented by the users own data. There are such computer programs in the public domain, e.g., the Bent program (Ref. 8) and the International Reference Ionosphere program (Ref. 9). There have also been attempts to characterize the global TEC behavior by a relatively simple semiempirical function fit to the mean of global ionospheric data, such as the work of Wu.[2] A comparison between ionospheric delay data obtained by dual-band (2.30 and 8.42 GHz) Very Long Baseline Interferometry (VLBI) data and Faraday rotation data mapped by the Wu method was given in Ref. 10.

In the planned DSN configuration, GPS receivers would take data continuously in the proximity of each DSN antenna. From the obtained ionospheric data, which covers only certain portions of the sky, the total ionospheric electron content in the direction of a space probe is then determined. Thus for the DSN, ionospheric models need only be local in contrast to global prediction methods. When the angular separation between the observed and predicted direction is very small, (<1 deg), then no ionospheric mapping is necessary, only the GPS transmitter offsets have to be removed.

Our knowledge about the value and the stability of GPS transmitter offsets is very cursory. GPS handbooks (Ref. 11) quote only a 1-$\sigma$ level of 1 to 1.5 ns for these offsets. We have some secondary information about the prelaunch values (private communication by J.A. Klobuchar, February 1985), and these values we designate as "semiofficial prelaunch" values. Due to the lack of proper information, we chose to estimate these offsets from the data itself (therefore the tasks 1, 4, and 5 described at the end of this section are not separable; they are included in a single least-squares estimation procedure).

In the following we proceed to describe the model used in our estimation procedure. We define the "ionospheric shell" as the collection of maxima of ionospheric electron density profiles over the globe; we assume this to be a sphere, and we use currently h = 350 km for its height above the mean sea level (Figs. 4 and 5). The longitudes and latitudes of the observation site and the ray-path intersect point on the ionospheric shell coincides only when the observation is made at zenith. Otherwise the terrestrial longitude and latitude of the intersect position, $\phi'$ and $\theta'$, are given by the following geometric transformation formulas

$$\sin\theta' = \sin\theta\cos\alpha + \cos\theta\cos A\sin\alpha \tag{1}$$

$$\sin(\phi' - \phi) = \sin\alpha\sin A / \cos\theta' \tag{2}$$

where the differential angle $\alpha$ between the observation and intersect position is determined by

$$\cos(\alpha + E) = \cos E / (1 + (h/R)) \tag{3}$$

and where $\theta$ and $\phi$ are the latitude and longitude of the observation site, $A$ and $E$ are the azimuth and elevation angle of the line-of-sight direction, and $R$ is the mean radius of Earth. After the transformation from unprimed to primed quantities, the longitude $\phi'$ is then transformed into the solar reference frame, $\phi' \rightarrow \phi_{shell}$, where the Earth-Sun axis corresponds to 0 deg longitude on the shell.

The total electron content is modeled for vertical directions on the shell, then we map the vertical to the line-of-sight total electron content by a mapping function $M(E)$. At our current accuracy requirement for the mapping function, it is sufficient to use the simple geometric slant ratio at the shell height $h$:

$$M(E) = [1 - (\cos E/(1 + h/R))^2]^{-1/2} \tag{4}$$

For the least-squares estimation of ionospheric content, currently we use a second-order polynomial in Sun-referenced and Earth-centered spherical coordinates. These coordinates are the above-mentioned shell latitude $\theta_{shell}$ and longitude $\phi_{shell}$ being offset by a reference latitude and longitude corresponding to the middle of the observing session, so that both coordinates are zero at the reference point (see Fig. 5). These coordinates are designated as $\bar{\theta}$ and $\bar{\phi}$ and through Eqs. (1) through (3) they have an implicit dependence on $E$ and $A$. The delays $\tau(E)$ then are modeled by the following expression:

$$\tau_i(E) = o_i + M(E)(c_1 + c_2\bar{\phi} + c_3\bar{\theta} + c_4\bar{\phi}^2 + c_5\bar{\phi}\,\bar{\theta} + c_6\bar{\theta}^2) \tag{5}$$

where $o_i$ is the sum of the offsets of $i$th GPS satellite and the receiver, and the polynomial in brackets represents the total vertical electron content. A least-squares fit applied for all observations can estimate the offsets and the six polynomial coefficients, $c_1$ through $c_6$.

Having the polynomial coefficient determined, we can now estimate TEC to an arbitrary line-of-sight direction. First, the intersect position on the ionospheric shell is determined by using Eqs. (1) through (3). Then, transforming the intersect position into $\bar{\phi}$ and $\bar{\theta}$ and substituting these values and $E$ into Eq. (5) with zero offset values, we obtain the predicted line-of-sight content. In summary, the local model consists of the following components:

[2]Wu, S. C., "Ionospheric Calibration for SEASAT Altimeter," Engineering Memorandum 315-34, 1977. Jet Propulsion Laboratory, Pasadena, California (JPL internal document).

(1) Removing of GPS transmitter offsets from the measured delays.

(2) Determining the effective intersect position of the ray path of GPS signals with the ionospheric shell in terrestrial coordinates.

(3) Transforming these terrestrial coordinates into the geocentric solar reference frame.

(4) Mapping the line-of-sight delays to the local vertical at the intersect point on the shell.

(5) Estimation of the total ionospheric vertical content over the whole sky corresponding to a reasonable observation period; it should be long enough to contain a sufficient number of observations but short enough for describing the ionospheric content by a local model. Our experience indicates that a period of 4 to 6 h is sufficient.

(6) Determining the effective intersect position of the ray path in the predicted direction with the ionospheric shell in terrestrial coordinates.

(7) Transforming these terrestrial coordinates of the intersect point into the geocentric solar reference frame.

(8) Mapping the estimated ionospheric vertical content at that shell position to the line-of-sight prediction.

In the next section we will present the currently available results of the estimation technique described in this section.

## III. Results

Present results are based upon the reduction of ionospheric data obtained from two SERIES experiments carried out by L.E. Young and the SERIES team. The first experiment includes 14 days of nighttime data at various California locations (with the exception of one observing session at Harvard, Texas) between 15 January and 2 February of 1984 (Ref. 12). The data were taken by two receivers simultaneously with station separations ranging from 13 to 1300 km. In these observations, the receiver calibrators were not used. The L1 and L2 P-code signals are delayed relative to each other in the SERIES receiver, resulting, in these experiments, in an uncalibrated variable receiver offset with a mean value of ~25 ns ($\sim 70 \times 10^{16}$ el/m$^2$). This offset is large compared to the nighttime ionospheric content of $\sim 4 \times 10^{16}$ el/m$^2$; thus this experiment provided a good testing ground for the offset estimation technique.

The second experiment includes 4 days of daytime data taken during 27 to 31 August 1984. One receiver was stationed at DSS 12, Goldstone, California, and the other at the National Bureau of Standards at Boulder, Colorado. Thus the two receivers were separated by about 1000 km. Both receivers were properly calibrated.

The average postfit rms scatter of all measurements is ~0.5 ns ($1.5 \times 10^{16}$ el/m$^2$). The average formal error for TEC is also ~0.5 ns, while the formal error for GPS transmitter offsets is ~0.2 ns. However, due to modeling errors, our current estimation algorithm can result in incorrect ionospheric content values and thus the actual error is bigger than the formal ones. Estimation of TEC of the same daytime reference region on the ionospheric shell by two receivers separated by ~1000 km indicates an average line-of-sight discrepancy of 2 ns. Thus, we place the magnitude of current systematic errors at the 2-ns level. This value corresponds to $6 \times 10^{16}$ el/m$^2$ in TEC units.

At nighttime the mean ionospheric content is spatially nearly homogeneous and small in value; thus modeling errors are less important and the systematic ionospheric mapping errors are smaller. Consequently, the total (receiver-plus-transmitter) offsets determined at night contain also smaller systematic errors. A comparison between the SERIES nighttime and the corresponding Goldstone Faraday data (Fig. 6) exhibits an rms difference of ~0.5 ns ($1.5 \times 10^{16}$ el/m$^2$).

Since in these data the sum of transmitter and variable receiver (of the order of 25 ns) offsets were estimated, the agreement with the Faraday measurements is a good indication of small systematic errors in the nighttime estimation. At the same time this comparison gives an indication of the absence of cycle ambiguities in the Faraday data itself. Another comparison was given earlier in Ref. 6. In that study the transmitter offsets were not estimated nor known, and the Faraday TEC data were mapped to the SERIES TEC data by the Bent algorithm, giving a typical vertical content difference of $\sim 5 \times 10^{16}$ el/m$^2$ for an assumed separation of 2 h from the closest approach at midmorning. This value is somewhat larger than our current systematic daytime error of $\sim 3 \times 10^{16}$ el/m$^2$ for the vertical electron content ($6 \times 10^{16}$ el/m$^2$ typical line-of-sight prediction error).

A representative result of the statistical fitting procedure is shown in Fig. 7. The symbols correspond to measured delays obtained from the P-code signals of GPS satellites identified by their Space Vehicle (SV) numbers. The solid lines are the result of the fit. In Fig. 8 the intersect trajectories of the lines of sight of observations with the ionospheric shell are shown. The numeric labels represent the elevation angle of observations.

The estimated GPS transmitter offsets are shown in Figs. 9 and 10. Figure 9 represents the nighttime solution including

the large variable receiver offsets, while Fig. 10 represents the daytime solution with a calibrated receiver. The differenced offsets between satellites do only weakly depend on the model and are independent of the receiver offsets. One can observe from these plots that differenced offsets between satellites have little scatter even when the day and nighttime observations are compared. Noting that the day and nighttime observations are 7 months apart, our preliminary conclusion is that the GPS transmitter offsets are relatively stable.

While the semiofficial prelaunch offsets agree in sign and order of magnitude with our results, the values are different as can be seen in Fig. 10. Since we do not have at present well-calibrated nighttime data available, we cannot directly compare our offset values with the semiofficial prelaunch values. As can be seen on the daytime plot, the offsets can jump from day to day, presumably due to systematic modeling errors. However, our measured differenced offsets between satellites are directly comparable to the differenced semiofficial prelaunch values between satellites and they disagree in value (see Fig. 10). If, for example, we compare the differenced offsets for the satellite pair SV 9 and SV 11, the discrepancy is almost 5 ns.

## IV. Discussion

Our results imply that the GPS P-code L1–L2 transmitter offsets can be determined by a least-squares estimation technique from the SERIES ionospheric data itself. At nighttime we can determine these offsets with a formal error of 0.2 ns. We can also estimate the line-of-sight total ionospheric electron content with a systematic error of 0.7 ns ($2 \times 10^{16}$ el/m$^2$) for nighttime and 2 ns ($6 \times 10^{16}$ el/m$^2$) for daytime. We plan to improve at least the static part of the mapping algorithm by using a more complex functional form for the ionospheric content and include the Bent program into our software and do further comparisons. We plan to analyze SERIES-X ionospheric delay data using differenced dual-band P-code and connected carrier-phase measurements. Recent phase-connected carrier delay data obtained by R. Neilan indicate the possibility of a sizable reduction of multipath errors. Such improvement would be very important, since omnidirectional antennas are planned to be used in the GPS-based calibration network. We should also point out that by using several GPS receivers, global ionospheric total electron content prediction, by mapping techniques similar to the one presented in this article, may become possible.

## Acknowledgments

The SERIES ionospheric data was provided by L. E. Young, and H. N. Royden provided the Faraday rotation data. We wish to express our appreciation to L. E. Young, D. W. Trask, H. N. Royden, and C. L. Thornton for the helpful discussions and suggestions.

# References


1. Green, D. W., Lam, V. W., and Royden, H. N., "Effects of the Charged Particle Environment on Voyager Navigation at Jupiter and Saturn," *AIAA/AAS Astrodynamic Conference*, Danvers, Massachusetts, 1980.

2. Yip, K. W., Winn, F. B., Reid, M. S., and Stelzried, C. T., "Decimeter Modeling of Ionospheric Columnar Electron Content at S-band Frequencies," in Proceedings of the Symposium on the Effect of the Ionosphere on Space Systems and Communications, Naval Research Laboratory, Washington, D. C., pp. 345-352, 1975.

3. Townes, S. A., "A Study of the Charged Particle Calibration Requirements for the Deep Space Network," *TDA Progress Report 42-75*, Jet Propulsion Laboratory, Pasadena, Calif., pp. 124-131, 1983.

4. MacDoran, P. F., Spitzmesser, D. J., and Buennagel, L. A., "SERIES: Satellite Emission Range Inferred Earth Surveying," in *Proceedings of the Third International Geodetic Symposium on Satellite Positioning*, Vol. 2, pp. 1143-1164, Las Cruces, New Mexico, 1982.

5. Buennagel, L. A., MacDoran, P. F., Neilan, R. E., Spitzmesser, D. J., Young, L. E., *Satellite Emission Range Inferred Earth Survey (SERIES) Project: Final Report on Research and Development Phase, 1979 to 1983*, JPL Publication 84-16, Jet Propulsion Laboratory, Pasadena, Calif., 1984.

6. Royden, H. N., Miller, R. B., Buennagel, L. A., "Comparison of NAVSTAR Satellite L-Band Ionospheric Calibrations With Faraday Rotation Measurements," *Radio Science*, Vol. 19, pp. 798-804, 1984.

7. Chapman, S., "The Absorption and Dissociative or Ionizing Effect of Monochromatic Radiation in an Atmosphere on a Rotating Earth," *Proc. Phys. Soc.* (London), Vol. 43, pp. 26-45, 1931.

8. Bent, R. B., Llewellyn, S. K., *Description of the 1965-71 Ionospheric Model Used in the Definitive System (DODS)*, DBA-Systems, Melbourne, Florida, 1970.

9. *International Reference Ionosphere -IRI 79*, Word Data Center A for Solar-Terrestrial Physics, Report UAG-82, Boulder, Colorado, 1981.

10. Scheid, J. A., "Comparison of the Calibration of Ionospheric Delay in VLBI Data by the Methods of Dual Frequency and Faraday Rotation," *TDA Progress Report 42-82*, Jet Propulsion Laboratory, Pasadena, Calif., pp. 11-23, 1985.

11. *Interface Control Document*, 03953, Space Division, Rockwell International Corporation, Downey, California, 1975.

12. Goad, C. C., Sims, M. L., and Young, L. E., "A Comparison of Four Precise Global Positioning System Geodetic Receivers," *IEEE Transactions on Geoscience and Remote Sensing*, Vol. GE-23, pp. 458-466, 1985.

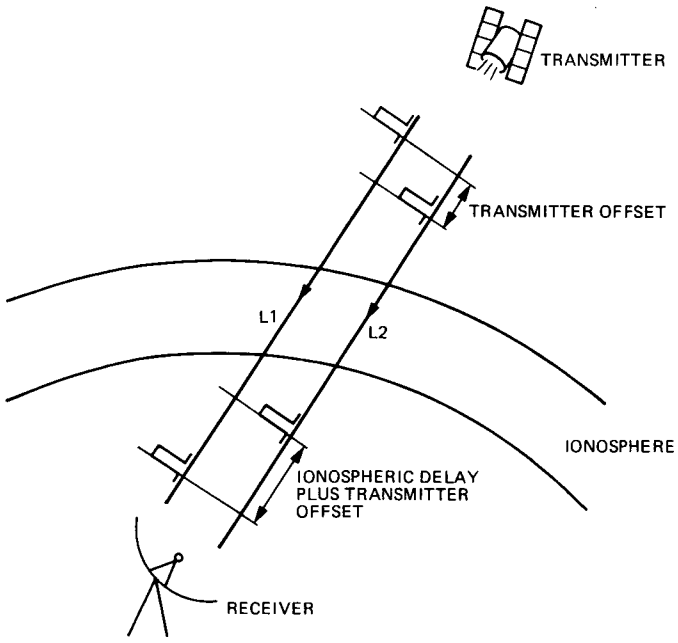


**Fig. 1. Schematic view of GPS-based ionospheric calibration**

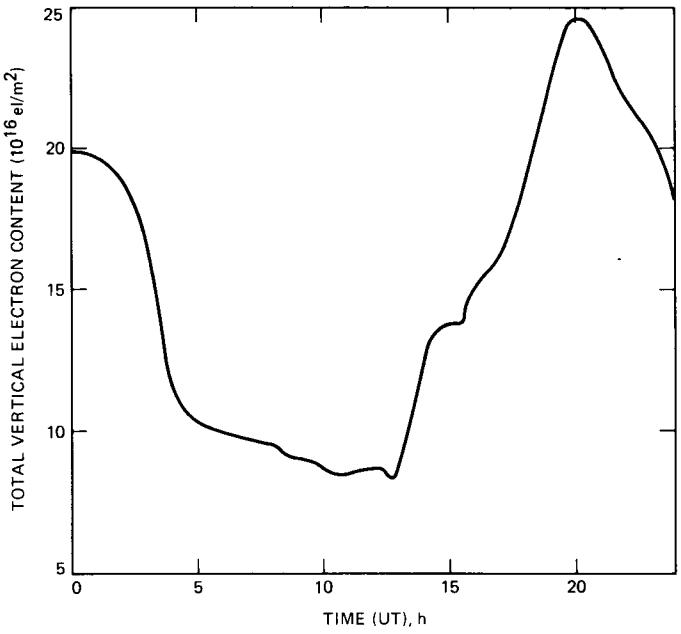


**Fig. 2. Typical daily variation of the total vertical electron content measured by Faraday rotation at Goldstone, California, on 30 August 1984**

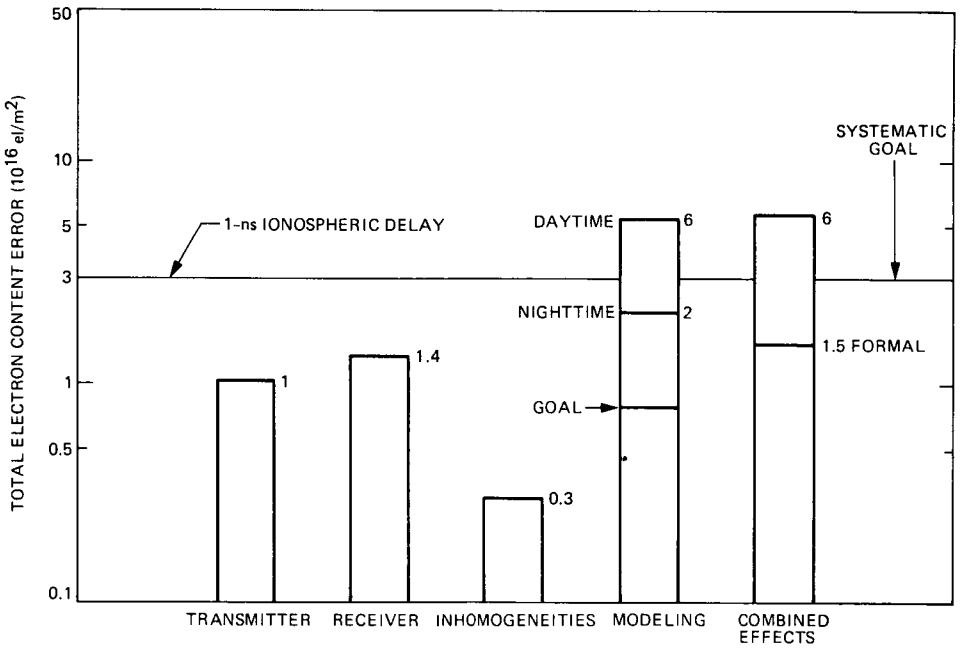


**Fig. 3. Error budget of ionospheric prediction of the line-of-sight total electron content**

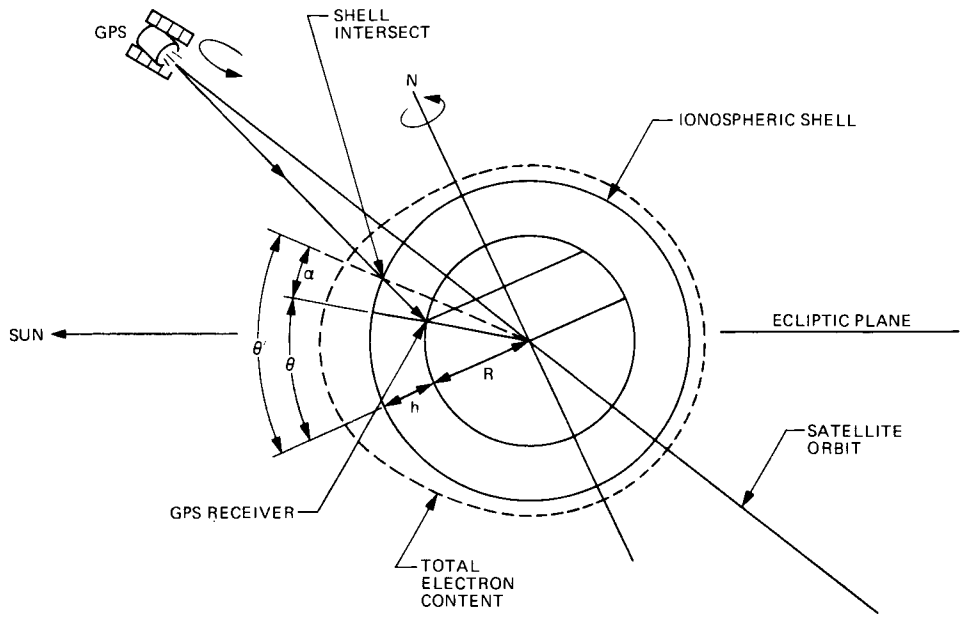


**Fig. 4. Geometry of the ionospheric modeling. The height *h* of the "ionospheric shell" is exaggerated. The dotted curve is a schematic representation of vertical TEC values**

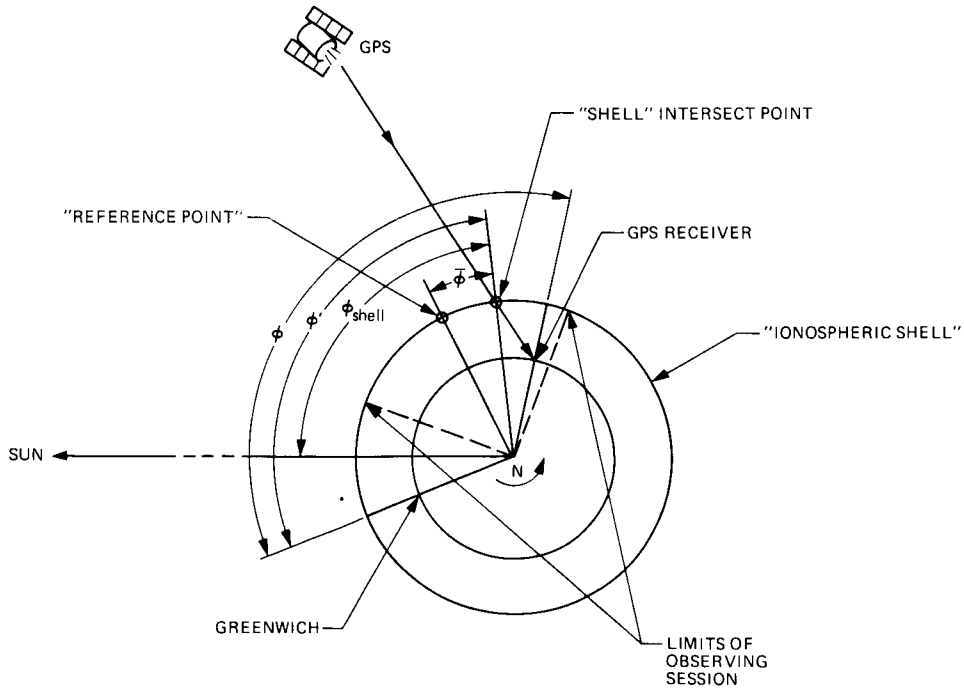


**Fig. 5. Schematic view of coordinate transformations. The longitude $\phi$ of the observation site is transformed into the relative geocentric solar coordinate $\bar{\phi}$**

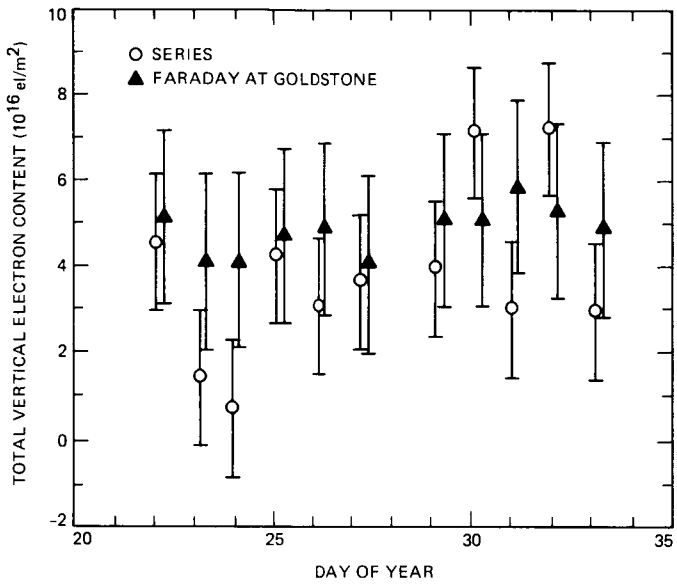


**Fig. 6. Comparison of SERIES with Faraday rotation data at nights of January 1984**

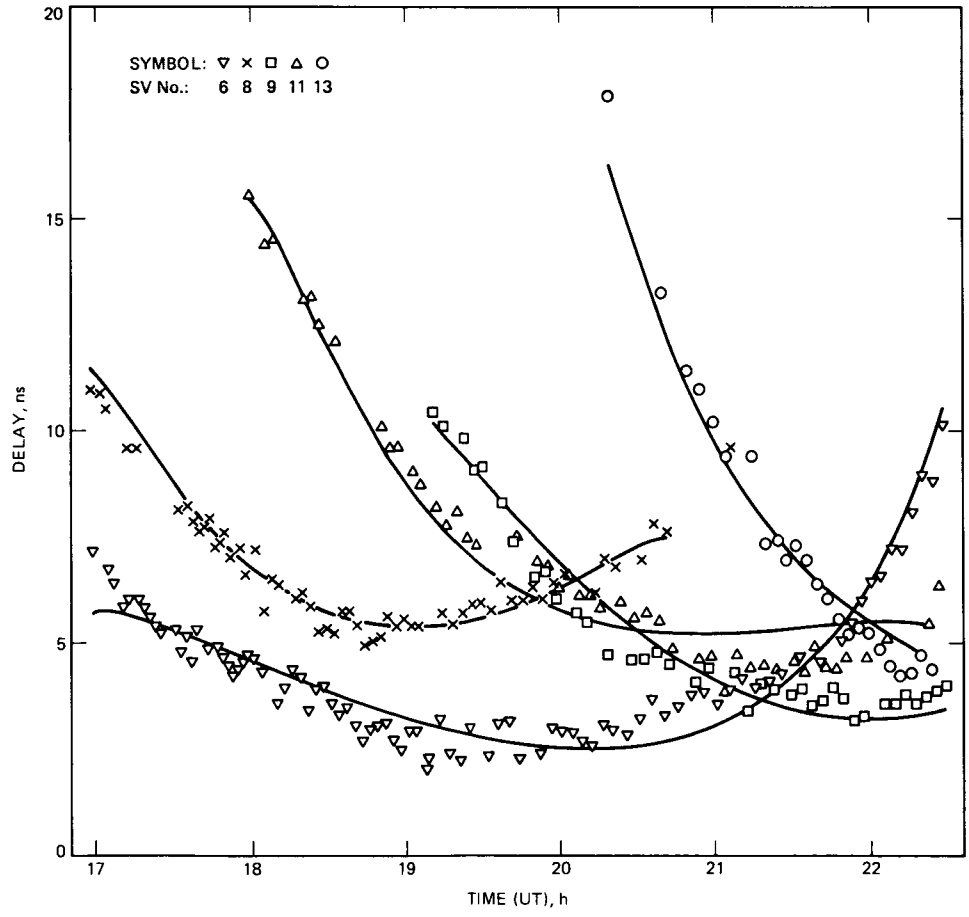


**Fig. 7. SERIES observation of total line-of-sight electron content. Data were taken at Goldstone, California, 30 August, 1984**

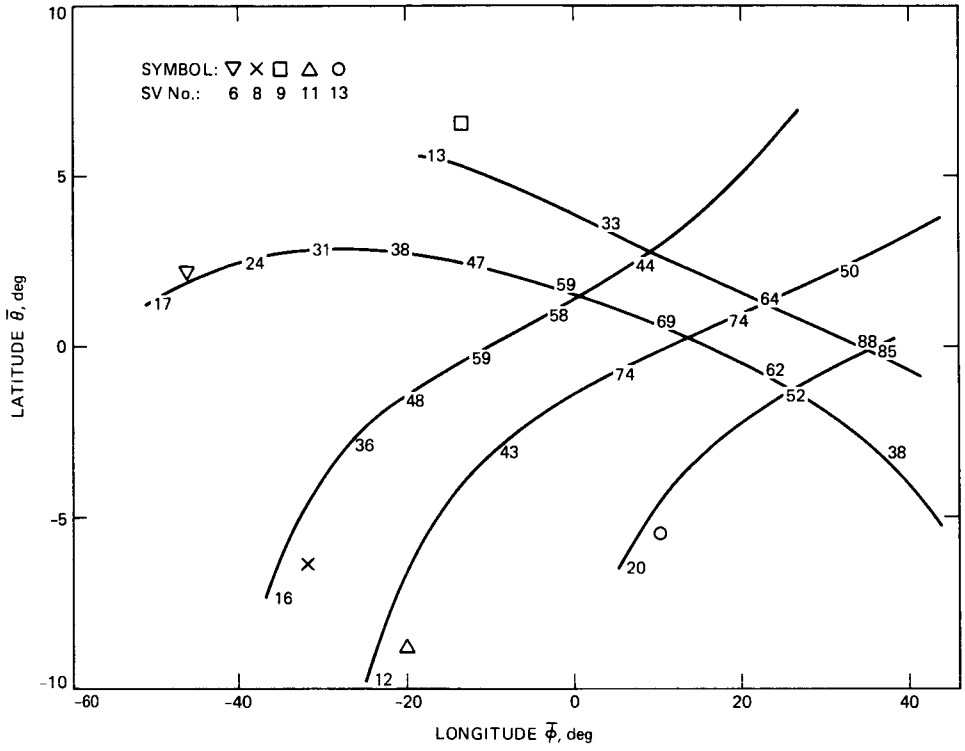


**Fig. 8. Intersects of the observed lines of sights with the ionospheric shell corresponding to figure 7. The numeric labels represent the elevation angles of observations. The origin of the coordinate system corresponds to 35.30 deg equatorial latitude and 359.14 deg longitude referenced to the Sun-Earth axis**

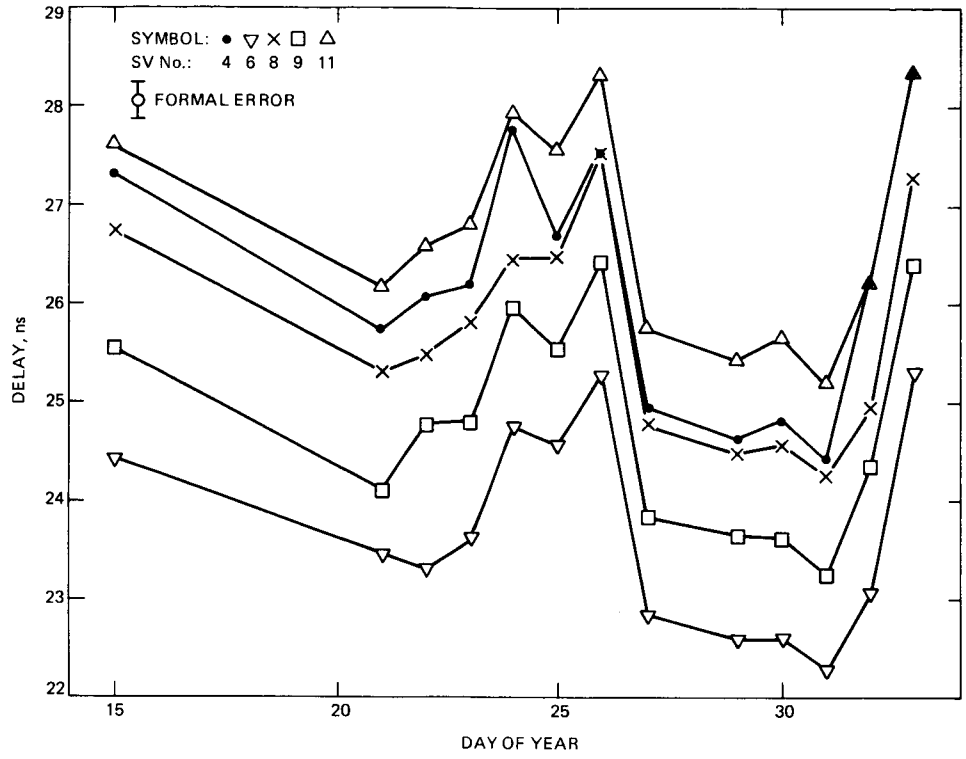


**Fig. 9. Sums of GPS transmitter and receiver P-code L1–L2 offsets determined from SERIES nighttime data. The data contains receiver offsets of the order of 25 ns**

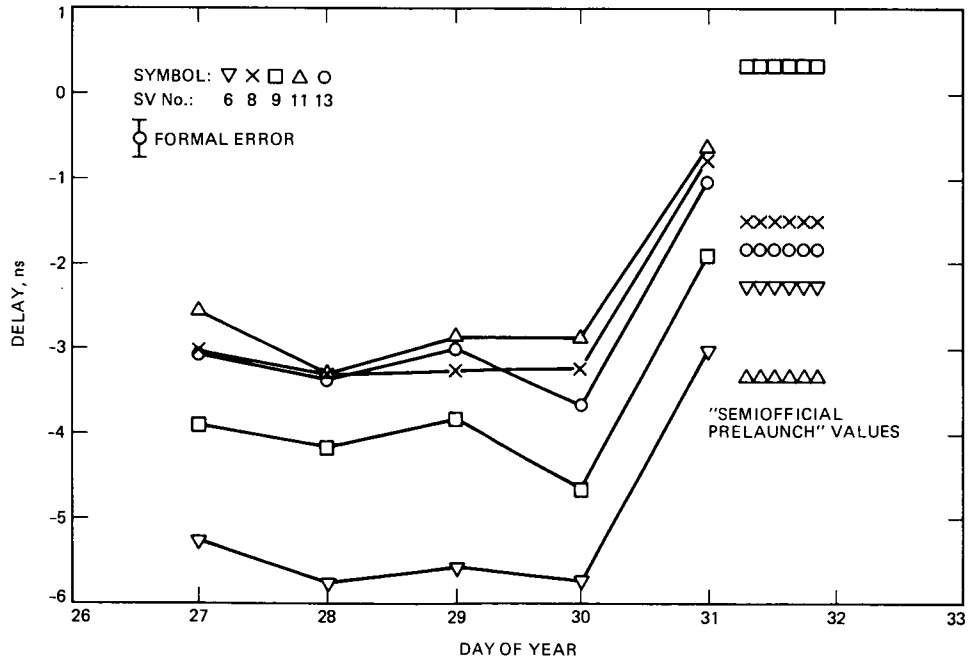


**Fig. 10. Sums of GPS transmitter and receiver P-code L1–L2 offsets determined from SERIES daytime data. The receiver is calibrated. The semiofficial prelaunch values are marked on the right side of the plot**

# Appendix A

# Instrumental Error Sources

1. **Transmitter errors.**

   (a) Multipath of radio signals by the satellite structure. The magnitude is unknown at present.

   (b) There is a time offset between the transmitted P-code signals at L1 and L2 frequencies. The value of this offset is different for each satellite. There are some semi-official prelaunch values for these offsets, though the official documentation quotes only an error estimate of 1.5 ns ($\sim 5 \times 10^{16}$ el/m$^2$) at 1 $\sigma$.

2. **Receiver errors.**

   (a) *System noise.* This is a negligible effect compared to the other listed errors, its value is ~0.04 ns.

   (b) *Temporal instabilities in the instrument.* The effect is ~0.1 ns.

   (c) Multipath of radio signals by ground objects; the multipath's estimated value is ~0.3 ns. We should note here that the SERIES receiver employs a directional antenna which should significantly reduce multipath relative to the omnidirectional antenna used by SERIES-X.

   (d) *GPS satellite interference in the receiver.* This effect is peculiar to the SERIES receiver, and occurs when more than one satellite appears in the beam pattern of the antenna. This error can be as high as 2 ns in magnitude. The observations corresponding to this effect were deleted from analysis.